The Canadian Mineralogist
Vol. 56, pp. 799-809 (2018)
DOI: 10.3749/canmin.1800032

BARWOODITE, $Mn^{2+}_6(Nb^{5+},\square)_2(SiO_4)_2(O,OH)_6$, A NEW MEMBER OF THE WELINITE GROUP FROM GRANITE MOUNTAIN, ARKANSAS

ANTHONY R. KAMPF[§] AND AARON J. CELESTIAN

Mineral Sciences Department, Natural History Museum of Los Angeles County, 900 Exposition Boulevard, Los Angeles, California 90007, USA

BARBARA P. NASH

Department of Geology and Geophysics, University of Utah, Salt Lake City, Utah 84112, USA

ABSTRACT

The new mineral barwoodite (IMA2017-046), $Mn^{2+}_6(Nb^{5+},\square)_2(SiO_4)_2(O,OH)_6$, was found in miarolitic cavities at the Big Rock quarry (also known as the 3M quarry), Granite Mountain, Little Rock, Pulaski County, Arkansas, USA. It is interpreted as crystallizing from pegmatitic fluids. The mineral occurs as brownish-red hexagonal plates up to 3 mm in diameter. Crystals are transparent with vitreous luster and light orange streak. The tenacity is brittle, the Mohs hardness is approximately 3½, the fracture is curved, and there is one perfect cleavage on {001}. The calculated density for the empirical formula is 4.227 g/cm^3. Barwoodite is optically uniaxial (–) with $\omega = 1.873(3)$ and $\varepsilon = 1.855(5)$ (white light) and is nonpleochroic. Electron microprobe analyses (WDS mode) provided the empirical formula $Mn^{2+}_6(Nb^{5+}_{0.94}Fe^{3+}_{0.18}Mn^{3+}_{0.11}\square_{0.77})_{\Sigma 2}(SiO_4)_2[O_{3.58}(OH)_{2.42}]_{\Sigma 6}$. The six strongest X-ray powder diffraction lines are [d_{obs} Å(I)(hkl)]: 3.125(95)($11\bar{1}$), 2.858(56)(021), 2.688(57)(210), 2.349(81)(300), 1.7930(100)(212), and 1.5505(75)($140,\bar{3}\bar{2}1$). Barwoodite is trigonal, $P3$, a 8.2139(10), c 4.8117(4) Å, V 281.14(7) Å^3, and $Z = 1$. The structure determination for barwoodite ($R_1 = 0.0246$ for 746 reflections with $I_o > 2\sigma I$) shows it to be isostructural with welinite, franciscanite, and örebroite. Together, these four minerals comprise the welinite group.

Keywords: barwoodite, new mineral, crystal structure, welinite group, Granite Mountain, Arkansas, USA.

INTRODUCTION

Welinite was first described from Langban, Sweden, by Moore (1967) and its structure was first determined by Moore (1969), who provided the formula $(Mn^{4+},W^{6+})_{<1}(Mn^{2+},W,Mg)_{<3}Si(O,OH)_7$. In 1986 Dunn *et al*. (1986) described the new minerals franciscanite and örebroite, showed them to be isotypic with welinite, and redefined welinite, providing the new ideal formula $Mn_6(W,Mg)_2Si_2(O,OH)_{\sim 14}$. While Dunn *et al*. (1986) based their findings on the reinterpretation of Moore's structure study, their model was confirmed by a new structure study in Pertlik (1986). Herein, we describe the new mineral barwoodite, which we have determined to be isostructural with welinite, franciscanite, and örebroite. As a consequence, we proposed that these four minerals be officially considered to constitute a mineral group and that it be called the welinite group, in light of the fact that welinite was the first member of the group to be described. It can be noted from a historical perspective that "chondrostibian", described from Sjögruvan, Hällefors, Örebro, Sweden, by Igelström (1893), has been shown to be dominantly örebroite with compositional zones of welinite (Holtstam 2001). The welinite group has now been approved by the Commission on New Minerals, Nomenclature and Classification (CNMNC) of the International Mineralogical Association.

The name barwoodite honors Dr. Henry ("Bumpi") L. Barwood (1947–2016), an American clay mineralogist (M.S., Auburn University) and surface chemist (Ph.D., Virginia Polytechnic Institute and State University, 1980). Dr. Barwood served as Professor

§ *Corresponding author e-mail address*: akampf@nhm.org

of Earth Science at Troy University (Troy, Alabama, USA) from 2002 to 2016. He served in industry and education throughout his career, authoring or coauthoring more than 60 research papers, articles, and published presentations.

Dr. Barwood was an avid mineral collector since childhood and, in later years, was particularly interested in rare micro-crystals. In the collecting community he was a pioneer in early, affordable, digital stacking photomicroscopy and 405 nm laser luminescence. He was also known for his expertise in visual and analytical identification of microminerals and was inducted into the Micromounters' Hall of Fame posthumously in 2017. Among his longtime collecting and research interests were phosphate minerals. In this area, for many years he collected wavellite samples from numerous localities and analyzed their fluorine contents. This culminated with his collaboration in the description of the new mineral fluorwavellite (Kampf *et al*. 2017). The manuscript for that publication was submitted only a few days before his death.

Dr. Barwood also was very interested in the rare minerals of alkaline rocks and particularly those of the Magnet Cove intrusive complex (Hot Springs County, Arkansas) and the Granite Mountain syenite (Little Rock, Arkansas; Barwood 1989). He made frequent collecting trips to these deposits with his lifelong collecting partner Robert W. Stevens. It was at the Big Rock quarry in the Granite Mountain syenite that they discovered the new mineral described herein. Dr. Barwood provided the specimens used in the description of the new mineral and gave permission for the mineral to be named in his honor. An obituary for Dr. Barwood was published recently by Stevens (2017).

The new mineral and name were approved by the Commission on New Minerals, Nomenclature and Classification (CNMNC) of the International Mineralogical Association (IMA2017-046). The description is based upon four cotype specimens deposited in the collections of the Natural History Museum of Los Angeles County, 900 Exposition Boulevard, Los Angeles, California 90007, USA, catalogue numbers 66634, 66635, 66636, and 66637.

Occurrence

The new mineral was discovered by Henry L. Barwood and Robert W. Stevens around 2005 at the Big Rock quarry (also known as the 3M quarry), Granite Mountain, Little Rock, Pulaski County, Arkansas (34°41′27′′N, 92°17′17′′W). The Big Rock quarry is one of numerous quarries on Granite Mountain, which is so named not for granite, but for the nepheline syenite pluton that the quarries exploit.

Fig. 1. Barwoodite plates with kupletskite (yellow) and aegirine (green) on quartz. Field of view is 1.7 mm across. Image by Henry Barwood.

Mining at the Big Rock quarry dates to the 1870s and the quarry is still actively producing crushed stone for various industrial and construction applications.

The best reference on the geology and mineralogy of the Granite Mountain syenite deposits is Barwood (1989). Research on the syenite, particularly in the 1970s and 1980s, revealed its petrographic complexity and the occurrences of a diversity of rare minerals. Most of the rare minerals have come from cavities in pegmatites and pegmatitic dikes. The only new mineral previously described from these deposits is eggletonite (Peacor *et al*. 1984), for which the Big Rock quarry is also the type locality. The new mineral barwoodite is found in miarolitic cavities in pegmatite in association with aegirine, albite, analcime, chamosite–pennantite, eggletonite, kupletskite, muscovite, natrolite, orthoclase, quartz, and zircon. Barwoodite is interpreted as crystallizing from pegmatitic fluids.

Physical and Optical Properties

Barwoodite occurs as plates to about 3 mm in diameter and 0.5 mm thick. The plates are typically in subparallel intergrowths extending wall-to-wall in small vugs and only rarely exhibit hexagonal outlines (Fig. 1). Intergrowths of plates usually contain included aegirine needles. Hexagonal plates exhibit the forms {100}, {010}, and {001}. Merohedral (racemic) twinning is indicated by the structure refinement. The mineral is brownish red with light orange streak and is nonfluorescent. Crystals are transparent and have vitreous luster. The mineral is brittle, with Mohs hardness of about 3½ based on

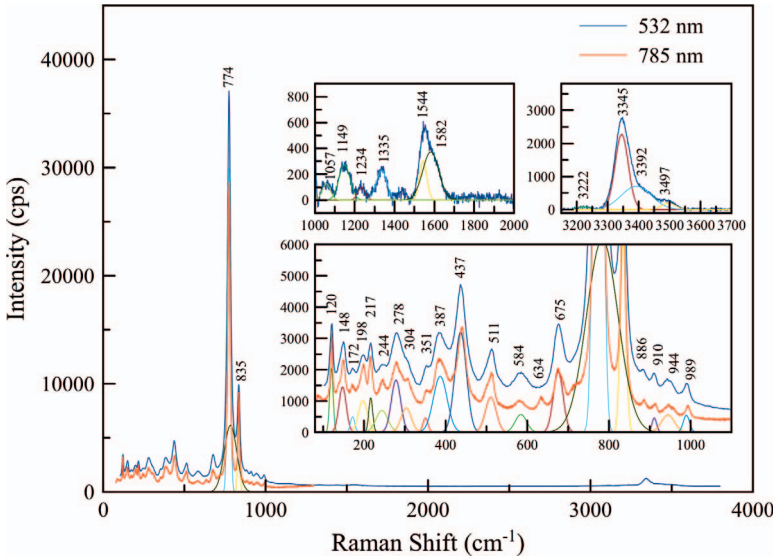

FIG. 2. Fitted Raman spectra of barwoodite. The top two inserts were collected separately (10 s 30×) to obtain better single:noise ratios.

scratch tests. The fracture is curved and there is one cleavage, perfect on {001}.

Efforts to accurately measure the density of the mineral in nearly saturated Clerici solution were unsuccessful because of difficulty in making observations in the murky, reddish, somewhat viscous solution; however, it was obvious that the density of the mineral was close to that of the solution (4.1–4.3 g/cm^3). The calculated densities for the empirical and ideal formulae are 4.227 and 4.168 g/cm^3, respectively.

Barwoodite is nonpleochroic and optically uniaxial (–) with $\omega = 1.873(3)$ and $\varepsilon = 1.855(5)$, measured in white light. The mineral loses color very slowly in dilute HCl and slowly in concentrated HCl at room temperature, but does not dissolve.

RAMAN SPECTROSCOPY

Crystals of barwoodite were placed on a polished Ni-metal surface and clamped to an automated XYZ microscope stage. Dispersive micro-Raman spectra were collected using a Horiba ExploRA PLUS instrument with a 532 nm laser, 1800 gr/mm diffraction grating, and 100 μm slit. The laser spot was approximately 1.2 μm in diameter and was focused on the sample through a 100× objective lens (N.A. 0.9). The barwoodite was not sensitive to the light and/or heat from the 532 nm laser; therefore, data were collected at 100% power. The spectrometer was calibrated using the 520.5 cm^{-1} line of a silicon standard. Data were collected from 80 to 4000 cm^{-1} for 3 s exposure with 10× averaging. The very strong 774 cm^{-1} peak prevented longer exposures due to detector saturation; therefore, additional spectra were collected to emphasize the 1000 to 2000 cm^{-1} and 3150 to 3700 cm^{-1} regions. Raman spectra peaks were fitted using a Gaussian shape function and are shown in Figure 2. The baseline was subtracted using a cubic spline. Our assignments for the Raman vibrational modes are provided in Table 1.

The barwoodite (this study) and franciscanite (RRUFF ID R060056) Raman spectra (Fig. 3) show distinctive similarities and differences. The overall patterns of both minerals have intense features around 780 cm^{-1}, with many weak peaks between 80 and 650 cm^{-1}. The peak around 1550 cm^{-1} is present in both barwoodite and franciscanite, and both have distinct OH-stretching modes above 3300 cm^{-1}. They differ in two important regions: the intense features around 780 cm^{-1} and the weaker features above 3300 cm^{-1}. Both barwoodite and franciscanite show four bands between 650 and 850 cm^{-1}; however, the franciscanite bands are less separated and less distinguishable than those in barwoodite, likely owing to the different octahedral site chemistry that, in turn, affects the SiO_4 and OH vibrational modes. In addition, franciscanite has a band at 2321 cm^{-1} that is not observed in the barwoodite spectrum. In the OH stretch region, franciscanite has a peak at 3426 cm^{-1} (likely

TABLE 1. ANALYSIS OF RAMAN VIBRATIONAL MODES FOR BARWOODITE

Raman shift (cm^{-1})	Relative intensity	Vibrational mode
120	w	lattice modes, ring breathing vibrations
148	w	
172	vw	
198	vw	
217	w	
244	vw	O–M_{oct}–O bending, octahedral deformation/rocking Si–O–Si bend Si–O–M_{oct} bend OH bend and rock (*cf.* brucite, silimanite, talc, and others)
278	w	
304	vw	
351	vw	
387	w	
437	w	M–OH deformations (*cf.* brucite 428 and 480 cm^{-1}, glaucophane 674 cm^{-1}) O–Si–O bend, (*cf.* cordierite, beryl). Note that 636 cm^{-1} is the SiO_4 symmetric stretch for talc 634 cm^{-1} peak only observed with 785 nm laser.
511	w	
584	w	
634	w	
675	w	
774	vs	OH deformation perpendicular to MnO layers (*cf.* brucite 782 cm^{-1}, glaucophane 674 cm^{-1}, adamite 812 cm^{-1}, hornblende 662 cm^{-1}) possibly SiO_4 symmetric stretch.
783	m	broad peak in this study, NbO_6 chain stretch (*cf.* titanite 782 cm^{-1}) and/or SiO_4 symmetric stretch
835	s	SiO_4 symmetric stretch (*cf.* titanite, forsterite, grossular, merwinite) OH out-of-plane bend (adamite, cummingtonite, hornblende). Note that the nesosilicate symmetric stretch (v_1) for SiO_4 has a wide range depending on connectivity, *e.g.*, ternesite – 812 cm^{-1}, forsterite – 819 cm^{-1}, ringwoodite – 829 cm^{-1}, norbergite – 842 cm^{-1}, titanite – 845 cm^{-1}, grossular – 848 cm^{-1}, merwinite – 858 cm^{-1}, willemite – 865 cm^{-1}, fresnoite – 959 cm^{-1}
886	w	O–Si–O asymmetric stretch Si–O–M asymmetric stretch (*cf.* quartz, silimanite,
910	w	forsterite, grossular, lintisite, clinoenstatite, tremolite, tugtupite, topaz) Si–O–Si
944	w	asymmetric stretch (*cf.* hornblende)
989	w	
1057	vw	
1149	vw	
1234	vw	OH deformation (*cf.* malachite) and H–O–H bend (*cf.* lintisite, antarcticite, kottigite,
1335	vw	lansfordite)
1544	vw	
1582	vw	
3222	w	OH stretching (*cf.* many minerals with molecular H_2O)
3345	w	
3392	w	
3497	w	

Only calculated data (from wurm.info; Caracas & Bobocioiu 2011) that closely matched measured data (from rruff.info; Lafuente *et al.* 2015) were used in this comparison. Intensity abbreviations: vw = very weak, w = weak, m = medium, s = strong, vs = very strong.

composed of multiple bands), while barwoodite modes are between 3222 and 3497 cm^{-1}. Without precise H positions being determined for barwoodite and franciscanite, it is difficult to quantify the OH vibrational differences with certainty.

Chemical Composition

Chemical compositions (12 points on six crystals) were determined at the University of Utah using a Cameca SX-50 electron microprobe with four wave-

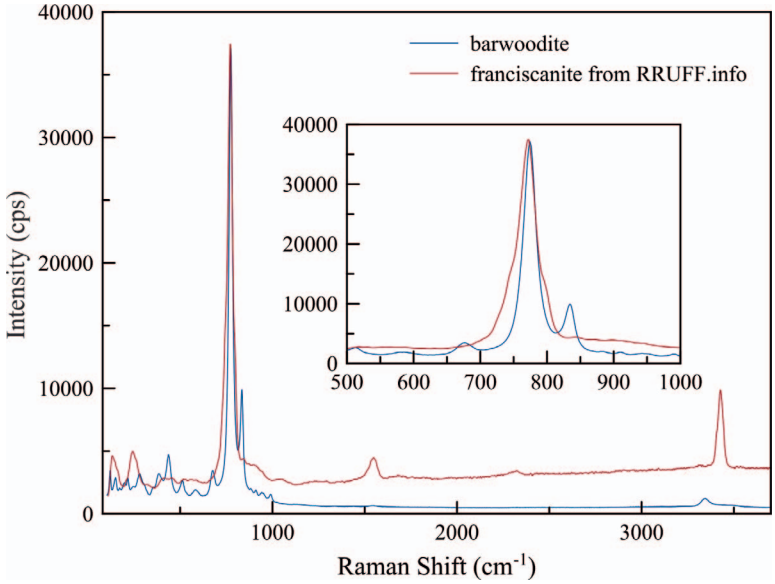

FIG. 3. Comparison of Raman spectra of barwoodite and franciscanite.

length-dispersive spectrometers and *Probe for EPMA* software. Analytical conditions were 15 kV accelerating voltage, 25 nA beam current, and a beam diameter of 10 μm. Barwoodite exhibited no obvious damage under the electron beam. Counting times were 20 s on peak and 10 s on + and − background. No other elements were detected by EDS. Other likely elements (including Ta, Ti, and Zr) were sought by WDS, but none were above the detection limits. Raw X-ray intensities were corrected for matrix effects with a $\phi(\rho z)$ algorithm (Pouchou & Pichoir 1991). The EPMA results indicated 6.11 Mn *apfu*; however, the Mn sites in the structure can only accommodate six Mn^{2+}, so the remaining 0.11 Mn *apfu* must be accommodated at the Nb sites as Mn^{3+}. Because insufficient material was available for a direct determination of H_2O, the amount of water was calculated on the basis of charge balance and O = 14 *apfu*, as determined by the crystal structure analysis (see below). Analytical data are given in Table 2.

The empirical formula is $Mn^{2+}_6(Nb^{5+}_{0.94}Fe^{3+}_{0.18}Mn^{3+}_{0.11}\square_{0.77})_{\Sigma 2}(SiO_4)_2[O_{3.58}(OH)_{2.42}]_{\Sigma 6}$. The simplified formula is $Mn^{2+}_6(Nb^{5+},\square)_2(SiO_4)_2(O,OH)_6$ and the endmember formula, assuming half occupancy of the Nb sites, is $Mn^{2+}_6Nb^{5+}(SiO_4)_2O_3(OH)_3$, which requires MnO 60.31, Nb_2O_5 18.83, SiO_2 17.03, H_2O 3.83, total 100 wt.%.

The Gladstone-Dale compatibility, $1 - (K_p/K_c)$, is 0.035 (excellent) for the empirical formula, 0.019 (superior) based upon the ideal formula, and 0.009 (superior) based upon the structural formula.

TABLE 2. ANALYTICAL DATA (IN wt.%) FOR BARWOODITE

Constituent	Mean	Range	Std. Dev.	Standard
MnO	[60.01]	59.34–60.77	0.46	rhodonite
MnO*	58.97			
Mn_2O_3*	1.21			
Fe_2O_3	1.96	1.77–2.08	0.11	hematite
Nb_2O_5	17.39	16.84–18.94	0.68	syn. $SrBaNb_4O_{10}$
SiO_2	16.65	16.44–16.96	0.18	rhodonite
H_2O§	3.02			
Total	99.20			

* Mn^{2+} and Mn^{3+} allocated according to assigned site occupancies.
§ Calculated on the basis of charge balance and O = 14 *apfu*.

TABLE 3. POWDER X-RAY DATA (*d* IN Å) FOR BARWOODITE

I_{obs}	d_{obs}	d_{calc}	I_{calc}	*hkl*	I_{obs}	d_{obs}	d_{calc}	I_{calc}	*hkl*
11	4.111	4.1070	16	1 1 0	23	1.6688	1.6681	16	$0\,\bar{4}\,\bar{1}$
34	3.994	3.9855	22	1 0 1	7	1.6311	1.6319	8	2 3 0
		3.5567	1	2 0 0			1.5646	5	1 0 3
95	3.125	3.1238	100	$1\,1\,\bar{1}$			1.5619	2	$\bar{2}\,\bar{2}\,2$
56	2.858	2.8602	68	0 2 1	75	1.5505	1.5523	47	1 4 0
57	2.688	2.6886	55	2 1 0			1.5455	22	$\bar{3}\,\bar{2}\,1$
14	2.403	2.4059	17	0 0 2			1.5256	1	3 1 2
		2.3711	13	3 0 0	7	1.4941	1.4940	9	$11\bar{3}$
81	2.349	2.3471	75	1 2 1	7	1.4647	1.4773	3	4 1 1
3	2.127	2.1269	5	0 3 1			1.4621	5	2 0 3
6	2.078	2.0759	5	1 1 2			1.4301	1	$\bar{4}\,0\,\bar{2}$
6	1.9847	1.9928	2	0 2 2	8	1.3775	1.3774	14	1 2 3
		1.9729	2	3 1 0			1.3505	3	2 3 2
		1.8887	3	$2\,2\,\bar{1}$	6	1.3456	1.3443	6	4 2 0
11	1.8256	1.8254	14	1 3 1			1.3285	1	0 3 3
100	1.7930	1.7929	96	2 1 2	3	1.3164	1.3167	6	$3\,3\,\bar{1}$
		1.7784	3	4 0 0	12	1.3037	1.3043	15	$\bar{1}\,\bar{4}\,\bar{2}$
8	1.6893	1.6888	14	3 0 2					

X-Ray Diffraction: Experimental

Powder X-ray studies were done using a Rigaku R-Axis Rapid II curved imaging plate microdiffractometer, with monochromatized Mo$K\alpha$ radiation (λ = 0.71075 Å). A Gandolfi-like motion on the φ and ω axes was used to randomize the samples. Observed *d* values and intensities were derived by profile-fitting using JADE 2010 software (Materials Data, Inc.). Data are given in Table 3. Unit-cell parameters refined from the powder data using JADE 2010 with whole-pattern fitting are *a* 8.2031(15), *c* 4.8088(9) Å, and *V* 280.24(12) Å^3.

Single-crystal data were collected using the same diffractometer and radiation noted above. The Rigaku CrystalClear software package was used for processing the structure data, including the application of an empirical absorption correction using the multi-scan method with ABSCOR (Higashi 2001). The structure was solved by direct methods using SIR2011 (Burla *et al*. 2012) and then atom coordinates were transformed and labelled to correspond to those in the structure of franciscanite (Pertlik 1986), with which the mineral is isostructural. SHELXL-2016 (Sheldrick 2015) was used for refinement of the structure. The refinement indicated the presence of merohedral (racemic) twinning, which was incorporated into subsequent refinement cycles, yielding a final Flack parameter of 0.61(5). The occupancies of two sites containing Nb refined to somewhat less than half occupancy by Nb (0.446 and 0.471). Difference-Fourier maps did not indicate the locations of possible H sites. Data collection and refinement details are given in Table 4, atom coordinates and displacement parameters in Table 5, selected bond distances in Table 6, and a bond valence analysis in Table 7. A CIF file that also contains observed and calculated structure factors has been deposited and is available from the Depository of Unpublished Data on the MAC website[1].

Atomic Arrangement of Minerals in the Welinite Group

The crystal structure of members of the welinite group (Fig. 4) is based on the hexagonal close-packing of oxygen atoms with the layer sequence A-B-A-B-A-

[1] Supplementary Data is available from the Depository of Unpublished data on the MAC website (http://mineralogicalassociation.ca/), document "Barwoodite, CM56, 18-00032".

TABLE 4. DATA COLLECTION AND STRUCTURE REFINEMENT DETAILS FOR BARWOODITE

Diffractometer	Rigaku R-Axis Rapid II
X-ray radiation / power	Mo$K\alpha$ ($\lambda = 0.71075$ Å)/50 kV, 40 mA
Temperature	293(2) K
Structural formula	$Mn^{2+}{}_6Nb^{5+}{}_{0.92}(SiO_4)_2O_{2.60}(OH)_{3.40}$
Space group	$P\bar{3}$
Unit cell dimensions	$a = 8.2139(10)$ Å
	$c = 4.8117(4)$ Å
V	281.14(7) Å^3
Z	1
Density (for above formula)	4.125 g cm^{-3}
Absorption coefficient	7.722 mm^{-1}
F(000)	331
Crystal size	100 × 70 × 30 μm
θ range	5.12 to 27.38°
Index ranges	$-8 \le h \le 8$, $-10 \le k \le 8$, $-6 \le l \le 6$
Refls. collected / unique	1843 / 856; $R_{int} = 0.025$
Reflections with $I > 2\sigma I$	746
Completeness to $\theta = 27.38°$	99.3%
Max. and min. transmission	0.801 and 0.512
Refinement method	Full-matrix least-squares on F^2
Parameters / restraints	76 / 0
GoF	1.028
Final R indices [$I_o > 2\sigma(I)$]	$R_1 = 0.0246$, $wR_2 = 0.0474$
R indices (all data)	$R_1 = 0.0302$, $wR_2 = 0.0486$
Flack parameter	0.61(5)
Extinction coefficient	0.008(3)
Largest diff. peak / hole	+0.87 / –0.43 e/A^3

* $R_{int} = \Sigma|F_o^2 - F_o^2(\text{mean})|/\Sigma[F_o^2]$. GoF $= S = \{\Sigma[w(F_o^2 - F_c^2)^2]/(n-p)\}^{1/2}$. $R_1 = \Sigma||F_o| - |F_c||/\Sigma|F_o|$. $wR_2 = \{\Sigma[w(F_o^2 - F_c^2)^2]/\Sigma[w(F_o^2)^2]\}^{1/2}$; $w = 1/[\sigma^2(F_o^2) + (aP)^2 + bP]$ where a is 0.0183, b is 0, and P is $[2F_c^2 + \text{Max}(F_o^2, 0)]/3$.

B along [001] and one A-B layer pair per unit cell. The close-packed arrangement contains four different voids that can be occupied by cations in octahedral coordination (M1a, M1b, M2a, and M2b) and two different voids that can be occupied by Si in tetrahedral coordination (Si1 and Si2). The M1a and M1b sites alternate along [001], yielding a chain of face-sharing octahedra. The M2a and M2b octahedra are each grouped in edge-sharing trimers; a single SiO_4 tetrahedron above the center of each trimer shares edges with each of the octahedra in the trimer, yielding a heteropolyhedral [$M2_3O_4(OH)_6(SiO_4)$] unit. These heteropolyhedral units link to one another by sharing octahedra–octahedra and octahedra–tetrahedra corners and they link to M1 octahedra in the chain by sharing octahedral edges, thereby forming a 3D framework.

The M2 sites in the structures of all four members of the welinite group are occupied predominantly by Mn^{2+}. The occupancies of the M1 sites (M1a and M1b being considered together) differentiate the four species from one another. In welinite, franciscanite, and barwoodite, the close approach of M cations in adjacent octahedra (~2.4 Å) is avoided because these sites are only approximately half-occupied: in welinite by W^{6+}, in franciscanite by V^{5+}, and in barwoodite by Nb^{5+}. In örebroite, the M sites are presumed to be alternately occupied (statistically) by Sb^{5+} and Fe^{3+}. The different endmember charge arrangements provided by the differing contents of the M1 sites require differing O:OH ratios in the formulae of each species to achieve electrostatic neutrality. This can be expressed by the general formula $M2^{2+}{}_6M1^{x+}{}_2(SiO_4)_2O_{(x-2)}(OH)_{(8-x)}$, where x is the total charge *pfu* of the cations at the M1 sites. The endmember formulae and reported cell parameters for the four members of the welinite group are provided in Table 8.

As noted above, the differentiation of the four current members of the welinite group is based upon the occupants of the M1 sites. The diverse cations that can occupy these sites, particularly in terms of their charges, and the necessity for offsetting vacancies for some cation substitutions make the chemical isomorphism within this group quite

TABLE 5. ATOM COORDINATES AND DISPLACEMENT PARAMETERS (Å^2) FOR BARWOODITE

	x/*a*	*y*/*b*	*z*/*c*	U_{eq}		
Mn1	0.58555(16)	0.89022(14)	0	0.0116(3)		
Mn2	0.41500(16)	0.10951(14)	0.5001(3)	0.0115(3)		
Nb1*	0	0	0.9657(5)	0.0090(8)		
Nb2*	0	0	0.4663(5)	0.0080(8)		
Si1	1/3	2/3	0.4377(7)	0.0085(7)		
Si2	2/3	1/3	0.9366(7)	0.0093(7)		
O2	0.3708(6)	0.8653(6)	0.2976(10)	0.0106(9)		
O22	0.6295(6)	0.1344(7)	0.7983(10)	0.0111(9)		
O3	1/3	2/3	0.7706(15)	0.0094(17)		
O33	2/3	1/3	0.2711(15)	0.0092(16)		
OH1	0.7798(6)	0.8321(6)	0.7752(11)	0.0130(11)		
OH11	0.2209(6)	0.1676(6)	0.2751(11)	0.0123(11)		
	U_{11}	U_{22}	U_{33}	U_{23}	U_{13}	U_{12}
Mn1	0.0136(8)	0.0107(8)	0.0108(5)	0.0014(5)	0.0024(4)	0.0063(6)
Mn2	0.0142(8)	0.0106(8)	0.0106(5)	–0.0009(5)	–0.0022(4)	0.0068(6)
Nb1	0.0078(11)	0.0078(11)	0.0113(12)	0	0	0.0039(5)
Nb2	0.0052(10)	0.0052(10)	0.0137(12)	0	0	0.0026(5)
Si1	0.0094(11)	0.0094(11)	0.0066(15)	0	0	0.0047(6)
Si2	0.0108(12)	0.0108(12)	0.0065(15)	0	0	0.0054(6)
O2	0.012(2)	0.009(2)	0.013(2)	0.0010(18)	0.0008(16)	0.006(2)
O22	0.012(2)	0.011(2)	0.011(2)	–0.0010(18)	–0.0019(16)	0.007(2)
O3	0.012(3)	0.012(3)	0.004(4)	0	0	0.0059(14)
O33	0.011(3)	0.011(3)	0.005(4)	0	0	0.0055(13)
OH1	0.011(3)	0.013(3)	0.010(2)	–0.0028(18)	–0.0009(17)	0.003(2)
OH11	0.011(3)	0.009(2)	0.015(2)	0.0038(18)	0.0037(17)	0.003(2)

* Refined occupancies: Nb1 = 0.446(5); Nb2 = 0.471(5)

TABLE 6. SELECTED BOND DISTANCES (Å) FOR BARWOODITE

Mn1–O22	2.091(5)	Nb1–OH1 (×3)	1.876(5)
Mn1–OH1	2.169(4)	Nb1–OH11 (×3)	2.215(5)
Mn1–O2	2.201(5)	<Nb1–O>	2.046
Mn1–OH11	2.223(5)		
Mn1–O3	2.253(4)	Nb2–OH11 (×3)	1.881(5)
Mn1–O2	2.367(4)	Nb2–OH1 (×3)	2.211(5)
<Mn1–O>	2.217	<Nb2–O>	2.046
Mn2–O2	2.092(5)	Si1–O3	1.602(7)
Mn2–OH11	2.168(4)	Si1–O2 (×3)	1.646(5)
Mn2–O22	2.201(4)	<Si1–O>	1.635
Mn2–OH1	2.223(5)		
Mn2–O33	2.251(4)	Si2–O33	1.610(8)
Mn2–O22	2.370(4)	Si2–O22 (×3)	1.645(5)
<Mn2–O>	2.218	<Si2–O>	1.636

intriguing. It is certainly possible that new members of this group will be discovered and that these new phases will reveal even greater diversity in the site substitutions. If a welinite-group phase containing Sb^{5+} half-occupying the *M*1 sites without significant Fe^{3+} or with a different cation approximately half-occupying the sites, it may qualify as a separate species. Hypothetically, this could also be the case

TABLE 7. BOND-VALENCE ANALYSIS FOR BARWOODITE (VALUES ARE EXPRESSED IN VALENCE UNITS*)

	Mn1	Mn2	Nb1	Nb2	Si1	Si2	sum
O2	0.33 0.22	0.43			0.95 ×3↓		1.93
O22	0.43	0.33 0.22				0.95 ×3↓	1.93
O3	0.29 ×3→				1.06		1.93
O33		0.29 ×3→				1.04	1.91
OH1	0.36	0.31	1.09 ×3↓ ×0.446→	0.44 ×3↓ ×0.471→			1.37
OH11	0.31	0.36	0.44 ×3↓ ×0.446→	1.08 ×3↓ ×0.471→			1.38
sum	1.94	1.94	4.59	4.56	3.91	3.89	

* The bond strengths are based upon assigned and refined cation occupancies from the structure refinement. Multiplicities and occupancies are indicated by ×↓→. Bond valence parameters are from Gagné & Hawthorne (2015). Hydrogen bonds are not included.

for other two-element combinations at the *M*1 sites. It is suggested that such potential phases be considered on a case-by-case basis, if they arise. Possible instances of cations other than Mn^{2+} dominantly occupying the *M*2 sites (*M*2a and *M*2b being considered together) would certainly qualify as distinct species. Because unrelated trivial names have already been applied to the four existing members of the welinite group, no proposal is made here for a unified approach for naming possible future members.

Acknowledgments

Associate Editor Frédéric Hatert is thanked for shepherding the manuscript through the review process and an anonymous reviewer is thanked for constructive comments on the manuscript. Robert W. Stevens and J. Adam Barwood are thanked for providing biographical background on Henry Barwood. This study was funded by the John Jago Trelawney Endowment to the Mineral Sciences Department of the Natural History Museum of Los Angeles County.

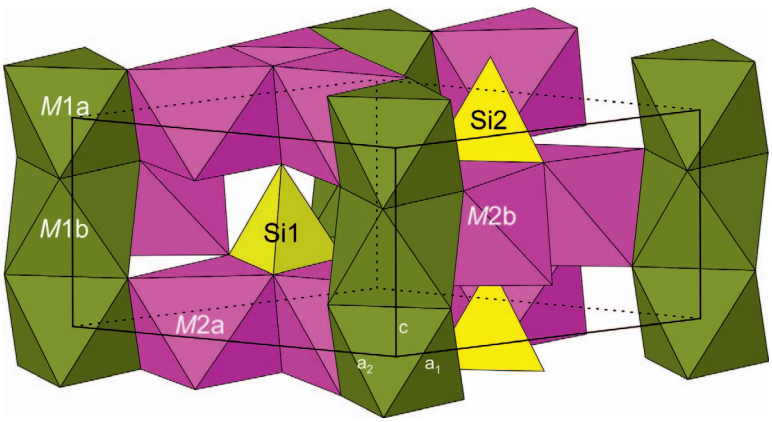

FIG. 4. Crystal structure of welinite-group minerals.

TABLE 8. COMPARISON OF BARWOODITE WITH FRANCISCANITE, OREBROITE, AND WELINITE

Mineral	Barwoodite	Franciscanite	Örebroite	Welinite
Formula	$Mn^{2+}{}_6(Nb^{5+},\square)_2(SiO_4)_2(O,OH)_6$	$Mn^{2+}{}_6(V^{5+},\square)_2(SiO_4)_2(O,OH)_6$	$Mn^{2+}{}_6(Sb^{5+},Fe^{3+})_2(SiO_4)_2(O,OH)_6$	$Mn^{2+}{}_6(W^{6+},Mg,\square)_2(SiO_4)_2(O,OH)_6$
Symmetry	Trigonal, *P*3	Trigonal, *P*3	Trigonal, *P*3	Trigonal, *P*3
Cell parameters	$a = 8.2139(10)$ Å	$a = 8.1518(3)$ Å	$a = 8.183(7)$ Å	$a = 8.155(7)$ Å
	$c = 4.8117(4)$ Å	$c = 4.8091(2)$ Å	$c = 4.756(9)$ Å	$c = 4.785(5)$ Å
V	281.14(7) Å^3	276.76(2) Å^3	275.8(5) Å^3	275.6(6) Å^3
Z	1	1	1	1
Reference	This study	Pertlik (1986), Dunn *et al.* (1986)	Dunn *et al.* (1986)	Moore (1967), Dunn *et al.* (1986)

References Cited

Barwood, H.L. (1989) Mineralogy of the Granite Mountain Syenite. *Rocks & Minerals* **64**, 314–322.

Burla, M.C., Caliandro, R., Camalli, M., Carrozzini, B., Cascarano, G.L., Giacovazzo, C., Mallamo, M., Mazzone, A., Polidori, G., & Spagna, R. (2012) *SIR2011*: a new package for crystal structure determination and refinement. *Journal of Applied Crystallography* **45**, 357–361.

Caracas, R. & Bobocioiu, E. (2011) The WURM project – a freely available web-based repository of computed physical data for minerals. *American Mineralogist* **96**, 437–443.

Dunn, P.J., Peacor, D.R., Erd, R.C., & Ramik, R.A. (1986) Franciscanite and örebroite, two new minerals from California and Sweden, related to redefined welinite. *American Mineralogist* **71**, 1522–1526.

Gagné, O.C. & Hawthorne, F.C. (2015) Comprehensive derivation of bond-valence parameters for ion pairs involving oxygen. *Acta Crystallographica* **B71**, 562–578.

Higashi, T. (2001) *ABSCOR*. Rigaku Corporation, Tokyo, Japan.

Holtstam, D. (2001) W and V mineralization in Långban-type Fe-Mn deposits: Epigenetic or syngenetic? *GFF* **123**, 29–33.

Igelström, L.J. (1893) Mineralogiska meddelanden. 19. Chondrostibian, ett nytt antimonmineral från Sjögrufvan, Grythytte socken, Örebro län. Geologiska Föreningens i Stockholm. *Förhandlingar* **15**, 343–344.

Kampf, A.R., Adams, P.M., Barwood, H., & Nash, B.P. (2017) Fluorwavellite, $Al_3(PO_4)_2(OH)_2F{\cdot}5H_2O$, the fluorine analogue of wavellite. *American Mineralogist* **102**, 909–915.

Lafuente, B., Downs, R.T., Yang, H., & Stone, N. (2015) The power of databases: the RRUFF project. *In* Highlights in Mineralogical Crystallography (T. Armbruster & R.M. Danisi, eds.). W. De Gruyter, Berlin, Germany (1–30).

Moore, P.B. (1967) Welinite, a new mineral from Långban. *Arkiv för Mineralogi och Geologi* **4**, 407–411.

Moore, P.B. (1969) The crystal structure of welinite, $(Mn^{4+},W^{6+})_{<1}(Mn^{2+},W,Mg)_{<3}Si(O,OH)_7$. *Arkiv för Mineralogi och Geologi* **4**, 459–466.

Peacor, D.R., Dunn, P.J., & Simmons, W.B. (1984) Eggletonite, the sodium analog of ganophyllite. *Mineralogical Magazine* **48**, 93–96.

Pertlik, F. (1986) The crystal structure of franciscanite, $Mn_3(V_x\square_{1-x})(SiO_4)(O,OH)_3, (x \sim 0.5)$. *Neues Jahrbuch für Mineralogie*, *Monatshefte* **1986**, 493–499.

Pouchou, J.-L. & Pichoir, F. (1991) Quantitative analysis of homogeneous or stratified microvolumes applying the model "PAP". *In* Electron Probe Quantitation (K.F.J. Heinrich & D.E. Newbury, eds.). Plenum Press, New York (31–75).

Sheldrick, G.M. (2015) Crystal structure refinement with SHELXL. *Acta Crystallographica* **C71**, 3–8.

Stevens, R.W. (2017) In Memoriam: Henry "Bumpi" L. Barwood (1947–2016). *Rocks & Minerals* **92**, 294–294.

Received May 9, 2018. Revised manuscript accepted August 8, 2018.